

## One-Electron Oxidation of Ruthenocene: Reactions of the Ruthenocenium Ion in Gentle Electrolyte Media

Jannie C. Swarts,<sup>\*†</sup> Ayman Nafady,<sup>‡</sup> John H. Roudebush, Sabrina Trupia, and William E. Geiger<sup>\*</sup>

Department of Chemistry, University of Vermont, Burlington, Vermont 05445

Received November 3, 2008

The electrochemical oxidation of ruthenocene, RuCp<sub>2</sub> (Cp = η<sup>5</sup>-C<sub>5</sub>H<sub>5</sub>), **1**, has been studied in dichloromethane using a supporting electrolyte containing either the [B(C<sub>6</sub>F<sub>5</sub>)<sub>4</sub>]<sup>-</sup> (TFAB) or the [B(C<sub>6</sub>H<sub>3</sub>(CF<sub>3</sub>)<sub>2</sub>)<sub>4</sub>]<sup>-</sup> (BARF<sub>24</sub>) counteranion. A quasi-Nernstian process was observed in both cases, with E<sub>1/2</sub> values of 0.41 and 0.57 V vs FeCp<sub>2</sub> in the respective electrolyte media. The ruthenocenium ion **1**<sup>+</sup> equilibrates with a metal–metal bonded dimer [Ru<sub>2</sub>Cp<sub>4</sub>]<sup>2+</sup>, **2**<sup>2+</sup>, that is increasingly preferred at low temperatures. Dimerization equilibrium constants determined by digital simulation of cyclic voltammetry (CV) curves were in the range of 10<sup>2</sup>–10<sup>4</sup> M<sup>-1</sup> at temperatures of 256 to 298 K. Near room temperature, and particularly when BARF<sub>24</sub> is the counteranion, the dinuclear species [Ru<sub>2</sub>Cp<sub>2</sub>(σ:η<sup>5</sup>-C<sub>5</sub>H<sub>4</sub>)<sub>2</sub>]<sup>2+</sup>, **3**<sup>2+</sup>, in which each metal is σ-bonded to a cyclopentadienyl ring, was the preferred electrolytic oxidation product. Cathodic reduction of **3**<sup>2+</sup> regenerated ruthenocene. The two dinuclear products, **2**<sup>2+</sup> and **3**<sup>2+</sup>, were characterized by <sup>1</sup>H NMR spectroscopy on anodically electrolyzed solutions of **1** at low temperatures in CD<sub>2</sub>Cl<sub>2</sub>/[NBu<sub>4</sub>][BARF<sub>24</sub>]. The variable temperature NMR behavior of these solutions showed that **3**<sup>2+</sup> and **2**<sup>2+</sup> take part in a thermal equilibrium, the latter being dominant at the lowest temperatures. Ruthenocene hydride, [1–H]<sup>+</sup>, was also identified as being present in the electrolysis solutions. The oxidation of ruthenocene is shown to be an inherent one-electron process, giving a ruthenocenium ion which is highly susceptible to reactions that allow it to regain an 18-electron configuration. In a dry non-donor solvent, and in the absence of nucleophiles, this electronic configuration is attained by self-reactions involving formation of Ru–Ru or Ru–C bonds. The present data offer a mechanistic explanation for the previously described results on the chemical oxidation of osmocene (Droege, M.W.; Harman, W.D.; Taube, H. *Inorg. Chem.* **1987**, *26*, 1309) and are relevant to the manner in which σ:η<sup>5</sup>-C<sub>5</sub>H<sub>4</sub>-complexes of other second and third-row metals are formed.

### Introduction

Although the overall chemical behavior of the heavier group 8 metallocenes is similar in many ways to that of ferrocene, the redox properties of the Ru and Os congeners differ greatly from that of the Fe complex. Ferrocene and the ferrocenium ion comprise an almost ideally reversible redox pair that has become the “TMS”<sup>1</sup> (TMS = tetramethylsilane) of nonaqueous reference potentials.<sup>2</sup> On the basis in large part of this idealized reversibility, the ferrocenyl group has found widespread use as a molecular “redox tag”

for the purpose of altering the chemical and analytical properties of target compounds.<sup>3</sup> In contrast, there is scant mention of similar applications of the ruthenocene or

<sup>\*</sup> To whom correspondence should be addressed. E-mail: swartsjc@sci.uovs.ac.za (J.C.S.), william.geiger@uvm.edu (W.E.G.).

<sup>†</sup> Permanent address: Department of Chemistry, University of the Orange Free State, Bloemfontein, 9300, Republic of South Africa.

<sup>‡</sup> Present address: School of Chemistry, Monash University, Clayton, Victoria 3800, Australia.

(1) TMS is the standard against which proton NMR chemical shifts are reported.

(2) (a) Gritzner, G.; Kuta, J. *Pure Appl. Chem.* **1984**, *56*, 461. (b) Connelly, N. G.; Geiger, W. E. *Chem. Rev.* **1996**, *96*, 877. (c) Geiger, W. E. *Organometallics* **2007**, *26*, 5738.

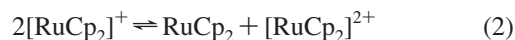
(3) Leading references may be found in (a) Cuffe, L.; Hudson, R. D. A.; Gallagher, J. F.; Jennings, S.; McAdam, C. J.; Connelly, R. B. T.; Manning, A. R.; Robinson, B. H.; Simpson, J. *Organometallics* **2005**, *24*, 2051. (b) Warren, S.; McCormac, T.; Dempsey, E. *Bioelectrochemistry* **2005**, *67*, 23. (c) Ryabov, A. D. *Adv. Inorg. Chem.* **2004**, *55*, 201. (d) Beer, P. D.; Hayes, E. *Coord. Chem. Rev.* **2003**, *240*, 167. (e) Chaubey, A.; Malhotra, B. D. *Biosens. Bioelectron.* **2002**, *17*, 441. (f) Suzawa, T.; Ikariyama, Y.; Aizawa, M. *Anal. Chem.* **1994**, *66*, 3889. (g) Hill, H. A. O.; Sanghera, G. S. In *Biosensor: A Practical Approach*; Cass, A. E. G., Ed.; Oxford University Press: London, 1990; pp 19–46. (h) Foulds, N. C.; Lowe, C. R. *Anal. Chem.* **1988**, *60*, 2473. (i) Cass, A. E. G.; Davis, G.; Francis, G. D.; Hill, H. A. O.; Aston, W. J.; Higgins, I. J.; Plotkin, E. V.; Scott, L. D. L.; Turner, A. P. F. *Anal. Chem.* **1984**, *56*, 667.

osmocene analogues,<sup>4</sup> in spite of there being some possible advantages with the heavier metals, including greater thermal stability and stronger cyclopentadienyl-to-metal bonding.<sup>5</sup> Reasoning that this disparity may be traced to the incompletely understood redox chemistry of ruthenocene and osmocene, we investigated the anodic behavior of RuCp<sub>2</sub> (Cp = η<sup>5</sup>-C<sub>5</sub>H<sub>5</sub>), **1**, under gentle medium conditions, and this paper offers a detailed view of the electrochemical production and chemical fate of the ruthenocenium ion when generated in the presence of a low-donor solvent and a weakly coordinating anion (WCA).

In the same historic paper<sup>6</sup> by Page and Wilkinson that described the electrochemistry of ferrocene, the anodic oxidation of ruthenocene was reported to be a reversible one-electron process at a mercury electrode. However, it was later shown that the isolated product, rather than being the ruthenocenium ion, was the Hg(I) adduct, Hg[Ru(Cp)<sub>2</sub>]<sup>+</sup>, formed by fast coupling of the initially produced Ru(III) species with the mercury being used as the anode.<sup>7</sup> On the basis of a number of attempts over the next couple of decades to find conditions under which the ruthenocenium ion is stable, it was generally concluded that it is unstable with respect to disproportionation, accounting for the Ru(IV) products often isolated after either the electrochemical<sup>8</sup> or the chemical<sup>9</sup> oxidation of **1**. On the basis of reactions such as shown in eq 1 it was generally concluded that the oxidation of ruthenocene was inherently a two-electron process. It should be noted that all of the electrochemical work was carried out in media that contained traditional



supporting electrolyte anions, either [PF<sub>6</sub>]<sup>-</sup>, [BF<sub>4</sub>]<sup>-</sup>, or [ClO<sub>4</sub>]<sup>-</sup>. Left unanswered was the question of why such a two-electron process should occur for a compound so much like ferrocene in its structural and electronic makeup.<sup>10</sup> Furthermore, a direct disproportionation of [RuCp<sub>2</sub>]<sup>+</sup> into RuCp<sub>2</sub> and [RuCp<sub>2</sub>]<sup>2+</sup> (eq 2) was not consistent with either



the results of Gale and Job, who found that the oxidation was a partially reversible one-electron process in molten salts,<sup>8a</sup> or the fact that the decamethylruthenocenium ion does not disproportionate.<sup>11</sup> The disclosure by Hill et al.<sup>12</sup> that the oxidation of ruthenocene was a simple one-electron processes in electrolyte solutions containing the WCA [B(C<sub>6</sub>H<sub>3</sub>(CF<sub>3</sub>)<sub>2</sub>)<sub>4</sub>]<sup>-</sup>, BArF<sub>24</sub>, suggested that the traditional anions were, in fact, responsible for promoting the two-electron ruthenocene oxidation process by anion attack at the strongly electrophilic Ru(III) center. However, the voltammetric data in ref 12 did not address the long-term (i.e., synthetic or electrolytic) fate of the ruthenocenium ion (1<sup>+</sup>). Ruthenocene initially became of interest to us when we fortuitously noticed a diminution of the chemical reversibility of its anodic oxidation at reduced temperatures in CH<sub>2</sub>Cl<sub>2</sub> containing [NBu<sub>4</sub>][TFAB] (TFAB = [B(C<sub>6</sub>F<sub>5</sub>)<sub>4</sub>]<sup>-</sup>) as supporting electrolyte, an effect which was amplified at increased concentrations of **1**. We hypothesized that the voltammetry was indicative of the generation of the bis(ruthenocenium) dication [Ru<sub>2</sub>Cp<sub>4</sub>]<sup>2+</sup>, **2**<sup>2+</sup>, and showed that this Ru–Ru bonded dimer was isolable as the TFAB salt by low-temperature (243 K) electrolysis.<sup>13</sup> It was also reported at that time that other products were produced in the electrolysis, becoming, in fact, the major products at ambient temperature. In the present paper we identify those electrolysis products and offer a coherent explanation of the complex oxidative behavior of ruthenocene.

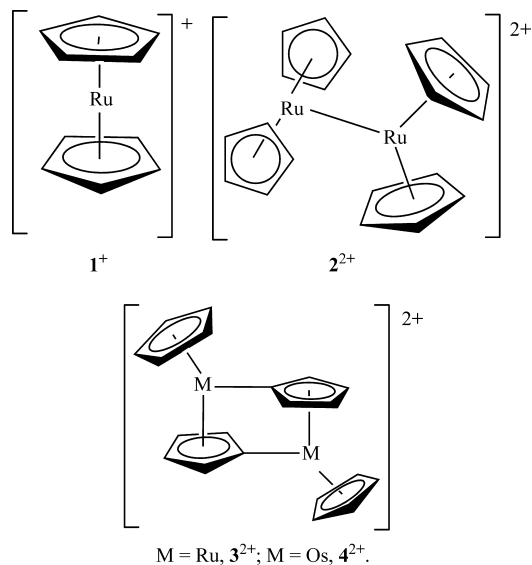
The present study is also relevant to literature on the oxidation of osmocene. Although Hill et al.<sup>12</sup> showed that it also followed one-electron stoichiometry with formation of [OsCp<sub>2</sub>]<sup>+</sup> in CH<sub>2</sub>Cl<sub>2</sub>/[NBu<sub>4</sub>][BArF<sub>24</sub>], dramatically different osmocene oxidation chemistry has been reported by Droege et al.<sup>14</sup> under other conditions. When oxidized by ceric ammonium nitrate in hot acetonitrile, osmocene gave the crystallographically characterized Os–Os bonded dimer [Os<sub>2</sub>Cp<sub>4</sub>]<sup>2+</sup> (*d*<sub>Os–Os</sub> = 3.038 Å), which served as the model for the Ru–Ru bonded dimer **2**<sup>2+</sup> reported earlier.<sup>13</sup> Warming the osmocenium dimer in nitromethane resulted in the formal loss of dihydrogen to give the dinuclear complex [Os<sub>2</sub>Cp<sub>2</sub>(σ:η<sup>5</sup>-C<sub>5</sub>H<sub>4</sub>)<sub>2</sub>]<sup>2+</sup>, **4**<sup>2+</sup>, in which each Os atom is both π-bonded and σ-bonded to a C<sub>5</sub>H<sub>4</sub> group. As will be shown below, an analogous dinuclear Ru complex, **3**<sup>2+</sup>, was observed at temperatures higher than 289 K which reverts to **2**<sup>2+</sup> in a thermally reversible process at substantially colder temperatures.

## Experimental Section

**Chemicals and Spectroscopy.** The compounds used or generated in this study were handled under strictly anaerobic (dinitrogen) conditions, with the exceptions of the air-stable compounds

- (4) See Wyman, I. W.; Robertson, K. N.; Cameron, T. S.; Swarts, J. C.; Aquino, M. A. S. *Organometallics* **2005**, *24*, 6055. for leading references.  
 (5) (a) Bennett, M. A.; Bruce, M. I.; Matheson, T. W. In *Comprehensive Organometallic Chemistry*; Wilkinson, G., Stone, F. G. A., Abel, E. W., Eds.; Pergamon Press: Elmsford, NY, 1982; Vol. 4, pp 759–767. (b) Adams, R. D.; Selegue, J. P. In *Comprehensive Organometallic Chemistry*; Wilkinson, G., Stone, F. G. A., Abel, E. W., Eds.; Pergamon Press: Elmsford, NY, 1982; Vol. 4, pp 1018–1020.  
 (6) Page, J.; Wilkinson, J. *J. Am. Chem. Soc.* **1952**, *74*, 6149.  
 (7) Hendrickson, D. N.; Sohn, Y. S.; Morrison, W. H., Jr.; Gray, H. B. *Inorg. Chem.* **1972**, *11*, 808. See also Morrison, W. H., Jr.; Hendrickson, D. N. *Inorg. Chem.* **1972**, *11*, 2912.  
 (8) (a) Gale, R. J.; Job, R. *Inorg. Chem.* **1981**, *20*, 42. (b) Denisovich, L. I.; Zakurin, N. V.; Bezrukova, A. A.; Gubin, S. P. *J. Organomet. Chem.* **1974**, *81*, 207. (c) Gubin, S. P.; Smirnova, L. I.; Denisovich, L. I.; Lubovich, A. A. *J. Organomet. Chem.* **1971**, *30*, 243. (d) Kuwana, T.; Bublitz, D. E.; Hoh, G. *J. Am. Chem. Soc.* **1960**, *82*, 5811.  
 (9) (a) Watanabe, M.; Sano, H. *Chem. Lett.* **1991**, 555. (b) Smith, T. P.; Kwan, K. S.; Taube, H.; Bino, A.; Cohen, S. *Inorg. Chem.* **1984**, *23*, 1943. (c) Sohn, Y. S.; Schlueter, A. W.; Hendrickson, D. N.; Gray, H. B. *Inorg. Chem.* **1974**, *13*, 301.  
 (10) Yamaguchi, Y.; Ding, W.; Sanderson, C. T.; Borden, M. L.; Morgan, M. J.; Kutal, C. *Coord. Chem. Rev.* **2007**, *251*, 515.

- (11) (a) Koelle, U.; Grub, J. *J. Organomet. Chem.* **1985**, *289*, 133. (b) Koelle, U.; Salzer, A. *J. Organomet. Chem.* **1983**, *243*, C27.  
 (12) Hill, M. G.; Lamanna, W. M.; Mann, K. R. *Inorg. Chem.* **1991**, *30*, 4687.  
 (13) Trupia, S.; Nafady, A.; Geiger, W. E. *Inorg. Chem.* **2003**, *42*, 5480.  
 (14) Droege, M. W.; Harman, W. D.; Taube, H. *Inorg. Chem.* **1987**, *26*, 1309.



ruthenocene (Strem Chemical, vacuum sublimed) and biruthenocene (gift from Dr. Masaru Sato, Saitama Univ). All electrochemical experiments were carried out in a Vacuum Atmospheres drybox having an oxygen content of 1–5 ppm. Reagent-grade dichloromethane was twice distilled from CaH<sub>2</sub>, the second distillation being carried out, bulb-to-bulb, under static vacuum. d<sub>2</sub>-Dichloromethane (CIL) was stored over type 4A molecular sieves before use. Glassware used for electrochemical experiments was cleaned by placing it in a No-Chromix (Godax Laboratories, Inc.) solution for at least 12 h, followed by copious rinsings with nanopure water and subsequent drying for at least 12 h in a 120 °C oven. The warm glassware was loaded into the drybox antechamber and allowed to cool under vacuum to minimize moisture contamination. [NBu<sub>4</sub>][PF<sub>6</sub>] (Acros) was thrice recrystallized from ethanol and vacuum-dried. [NBu<sub>4</sub>][TFAB] (TFAB = [B(C<sub>6</sub>F<sub>5</sub>)<sub>4</sub>]<sup>-</sup>), and [NBu<sub>4</sub>][BArF<sub>24</sub>] (BArF<sub>24</sub> = [B(C<sub>6</sub>H<sub>3</sub>(CF<sub>3</sub>)<sub>2</sub>)<sub>4</sub>]<sup>-</sup>) were prepared as previously described<sup>15</sup> through the metathesis of alkali metal salts obtained from Boulder Scientific Co., Boulder, Colorado. IR spectra were recorded with an ATI-Mattson Infinity Series FTIR interfaced to a computer employing Winfirst software at a resolution of 4 cm<sup>-1</sup>, and NMR spectra were recorded using a Bruker ARX 500 MHz spectrometer. Elemental analyses were performed by Robertson Laboratories.

**Electrochemistry.** A standard three-electrode cell configuration was employed in conjunction with a PARC 273A potentiostat interfaced to a personal computer through homemade software. The temperature of the electrochemical experiment was regulated by means of a cooling bath capable of controlling solution temperatures to about 1 °C.

Voltammetry scans were recorded using a glassy carbon working electrode disk of either 1 mm or 2 mm diameter (Bioanalytical Systems), the effective areas of which were checked by chronoamperometry on ferrocene in acetonitrile/0.1 M [NBu<sub>4</sub>][PF<sub>6</sub>] (diffusion coefficient = 2.4 × 10<sup>-5</sup> cm<sup>2</sup> s<sup>-1</sup>).<sup>16</sup> The disks were pretreated using a sequence of polishing with Buehler diamond paste of decreasing sizes (3 to 0.25 μm) interspersed by washings with nanopure water, and final vacuum drying. Bulk electrolyses were carried out in a three-compartment “H-type” cell having counter and working compartments separated by a fine glass frit. In this case, the working electrode was a basket-shaped Pt gauze which

had been treated with nitric acid, washed copiously with distilled water, and dried by first leaving it overnight at 120 °C, followed by evacuation. Potentials in this paper are referred to the ferrocene/ferrocenium reference couple.<sup>2</sup> Mechanistic aspects of redox reactions were probed by applying the appropriate diagnostic criteria to cyclic voltammetry (CV) data, using procedures described elsewhere,<sup>17</sup> and by digital simulations. Digital simulations of the CV data for ruthenocene were performed using Digisim 3.0 (Bioanalytical Systems). In the simulations, the fits for the irreversible cathodic wave for the reduction of 2<sup>2+</sup> at about -0.1 V were not made with the intention of getting a unique set of values. The fact that the wave arises from an electrochemically irreversible overall two-electron process precludes finding such a set with the experimental data available. The cathodic wave for the reduction of 2<sup>2+</sup> was therefore calculated based on an E<sub>irrev</sub>E<sub>qrev</sub> (q<sub>rev</sub> = quasi-reversible) model simply for the purpose of showing one set of charge-transfer parameters that could account for the observed cathodic wave shape.

**Electrosynthesis of [Ru<sub>2</sub>Cp<sub>4</sub>][B(C<sub>6</sub>F<sub>5</sub>)<sub>4</sub>]<sub>2</sub>.** Twenty-eight milligrams of RuCp<sub>2</sub> dissolved in 10 mL of CH<sub>2</sub>Cl<sub>2</sub>/0.05 M [NBu<sub>4</sub>][TFAB] was electrolyzed at 243 K (E<sub>appl</sub> = 0.8 V). After passage of about 1 F, a light yellow precipitate formed, which was filtered off while keeping the solution cold. The solid was washed twice with cold CH<sub>2</sub>Cl<sub>2</sub> to remove any supporting electrolyte or unreacted starting material and then vacuum-dried to give 67–77 mg (60–70%) of analytically pure [2][B(C<sub>6</sub>F<sub>5</sub>)<sub>4</sub>]<sub>2</sub>.

**Electrolysis/NMR Experiments.** Bulk electrolyses for <sup>1</sup>H NMR analyses were performed on 2–4 mL CD<sub>2</sub>Cl<sub>2</sub> solutions of ruthenocene (ca. 8–15 mM) and [NBu<sub>4</sub>][BArF<sub>24</sub>] (ca. 4 times in excess over ruthenocene) by applying a potential of 1.2V at 233 K. Owing to the lower solution volumes of these electrolyses, the cell employed a Pt gauze working electrode wrapped around two glass tubes fused with E-grade sintered glass at the tips and immersed into a holder with 7 mL capacity. Into one tube was immersed a Pt wire that served as cathode, with the other containing a Ag/AgCl reference electrode. The low electrolyte concentration of 30–40 mM was chosen to allow proper shimming of the NMR and to minimize chances that the butyl-cation signals might obscure the peaks of oxidation products. These conditions caused long electrolyses times, taking up to 90 min to reach the coulomb count expected for a one-electron process, but even then the current did not always approach zero, sometimes retaining as much as 20% of the initial value. Clearly over this longer time scale, the oxidation of ruthenocene gives one or more oxidizable side products (the light red tint observed at longer electrolysis times was indicative of some over-oxidation to a Ru(IV) species, and the text should be consulted for a fuller discussion of the coulometry, which attained the expected one-electron value under more standard electrolysis conditions). Samples for <sup>1</sup>H NMR spectra were removed from the electrolysis cell as 0.8 mL aliquots into NMR tubes, which were capped, removed from the glovebox, placed briefly in finely crushed dry ice, and put into the NMR probe at 233 K. Care was taken to remove frost from the outside of the NMR tube prior to loading.

## Results and Discussion

**Electrochemistry on Voltammetric Time Scale. I. With Weakly-Coordinating Anion Electrolytes.** As demonstrated in two earlier papers, the anodic oxidation of ruthenocene

(15) LeSuer, R. J.; Buttolph, C.; Geiger, W. E. *Anal. Chem.* **2004**, *76*, 6395.

(16) Hershberger, J. W.; Klingler, R. J.; Kochi, J. K. *J. Am. Chem. Soc.* **1983**, *105*, 61.

(17) Geiger, W. E. In *Laboratory Techniques in Electrochemistry*, 2nd ed.; Kissinger, P. T., Heineman, W. R., Eds.; Marcel Dekker: New York, 1996; Chapter 23.

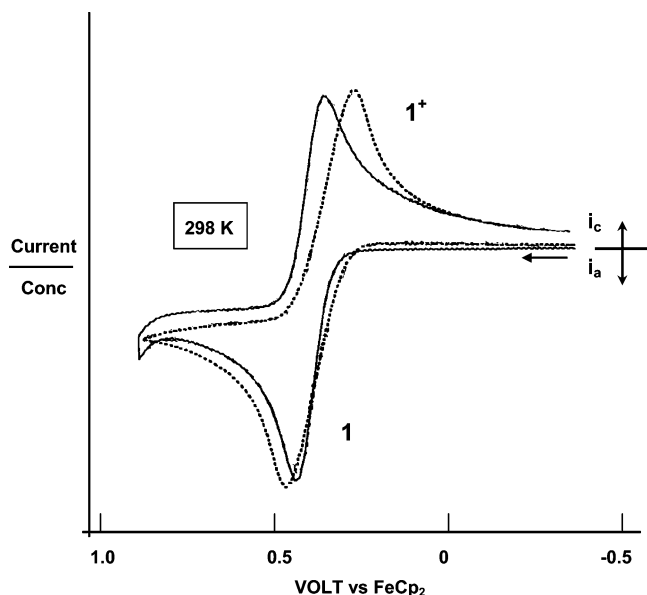


**Figure 1.** Cyclic voltammograms of different concentrations of ruthenocene in  $\text{CH}_2\text{Cl}_2/0.1 \text{ M } [\text{NBu}_4][\text{TFAB}]$ , utilizing a 2 mm glassy carbon working electrode at 298 K and  $0.1 \text{ V s}^{-1}$ . Solid line, 0.22 mM **1**, dotted line 5.2 mM **1**. Y-axis is current normalized for concentration.

**Table 1.**  $E_{1/2}$  Values of Ruthenocene and Osmocene and Differences Between Their Ionization Potentials and That of Ferrocene

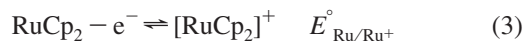
compound	medium <sup>a</sup>	$E_{1/2}$ vs FcH	$\text{IP} - \text{IP}(\text{FcH})^b$	reference
$\text{RuCp}_2$ , <b>1</b>	$\text{CH}_2\text{Cl}_2/0.1 \text{ M TFAB}$	0.41 V	0.57 eV	this work
$\text{OsCp}_2$	$\text{CH}_2\text{Cl}_2/0.1 \text{ M TFAB}$	0.25 V	0.27 eV	22
$\text{RuCp}_2$ , <b>1</b>	$\text{CH}_2\text{Cl}_2/0.05 \text{ M BArF}_{24}$	0.56 V	0.57 eV	12, this work
$\text{OsCp}_2$	$\text{CH}_2\text{Cl}_2/0.05 \text{ M BArF}_{24}$	0.36 V	0.27 eV	12

<sup>a</sup> Counterion is  $[\text{NBu}_4]^+$ ; TFAB =  $[\text{B}(\text{C}_6\text{F}_5)_4]^-$ ; BArF<sub>24</sub> =  $[\text{B}(\text{C}_6\text{H}_3(\text{CF}_3)_2)_4]^-$ .

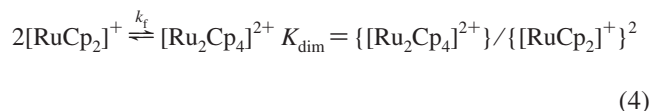
<sup>b</sup> Ionization potentials taken from ref 21.

displays a voltammetric response that is consistent in appearance with the simple reversible formation of ruthenocenium ion (eq 3) when carried out in a low-donor solvent and with a supporting electrolyte anion that is weakly coordinating.<sup>12,13</sup>

**IA.**  $[\text{B}(\text{C}_6\text{F}_5)_4]^-$ . When recorded at room temperature in  $\text{CH}_2\text{Cl}_2/[\text{NBu}_4][\text{TFAB}]$ ,



CV scans of **1** at lower scan rates had a quasi-Nernstian appearance, giving little hint of a dimerization process following electron transfer (eq 4), even at high



concentrations (Figure 1). The  $E_{1/2}$  value was 0.41 V versus FcH in this medium (see Table 1). At lower temperatures and/or faster scan rates, however, the wave lost some or all of its chemical reversibility, and a new broad cathodic product wave appeared (Figure 2) at more negative potentials (e.g.,  $E_{\text{pc}} = -0.06 \text{ V}$  at 243 K,  $\nu = 0.2 \text{ V s}^{-1}$ ). The fact that this effect was accentuated at higher concentrations of **1** was the basis on which the new product wave was assigned to the bis(ruthenocenium) dication  $2^{2+}$ ,<sup>13</sup> which was assumed to have a direct metal–metal bond by analogy to the

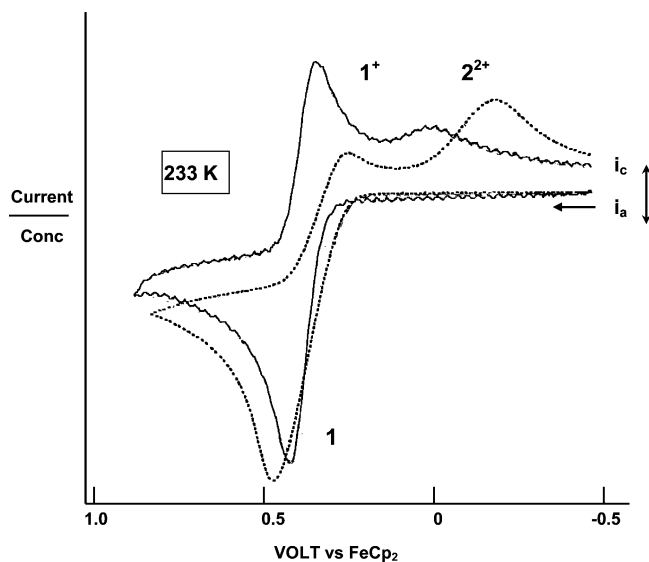
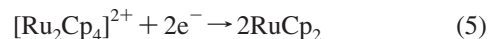


**Figure 2.** Cyclic voltammograms of different concentrations of ruthenocene in  $\text{CH}_2\text{Cl}_2/0.1 \text{ M } [\text{NBu}_4][\text{TFAB}]$ , 2 mm glassy carbon, 233 K,  $0.1 \text{ V s}^{-1}$ . Solid line, 0.22 mM **1**, dotted line 5.2 mM **1**. Y-axis is current normalized for concentration.

corresponding osmium compound.<sup>14</sup> Figure 2 shows the CV responses at 233 K for two different concentrations of **1**. Although the 5.2 mM scan (dotted line) shows ohmic error, it clearly demonstrates that the follow-up reaction of  $1^+$  increases with concentration, compelling the designation of the ruthenocene oxidation as an  $\text{EC}_{\text{dim}}$  mechanism (eqs 3 and 4). The fact that the CV curves at room temperature have quasi-Nernstian shapes (Figure 1) shows that the dimerization process is fast and reversible at that temperature on the CV time scale of several seconds. As described below, bulk anodic electrolysis of **1** at low temperatures allowed the isolation of the dimer dication  $2^{2+}$  as a *bis*-TFAB salt.

The electrochemical irreversibility of the reduction of  $2^{2+}$ , which was confirmed by application of appropriate diagnostics to the scan-rate dependent shape and position of the wave,<sup>17</sup> has ample precedent in the cathodic behavior of other unbridged metal–metal bonded systems, which invariably results in efficient formation of the 18-electron mononuclear “parent” complex.<sup>18</sup> In the present case, the reduction of  $2^{2+}$  regenerates ruthenocene (eq 5), as confirmed by bulk electrolysis at low temperatures (*vide infra*).



Digital simulations were carried out for comparison with the experimental CV curves obtained at a number of different temperatures (243 to 298 K), scan rates ( $0.2$  to  $2.0 \text{ V s}^{-1}$ ), and concentrations of **1** (1 to 5 mM). Although reasonably satisfactory matches were obtained for an  $\text{E}_{\text{rev}}\text{C}_{\text{dim}}$  anodic process (eqs 3 and 4) followed by an  $\text{E}_{\text{irrev}}\text{E}$  cathodic process

- (18) (a) Pugh, J. R.; Meyer, T. J. *J. Am. Chem. Soc.* **1992**, *114*, 3784. (b) Kukhareno, S. V.; Bezrukova, A. A.; Rubezhov, A. Z.; Strelets, V. V. *Metalloorg. Khim.* **1990**, *3*, 634. (c) Lacombe, D. A.; Anderson, J. E.; Kadish, K. M. *Inorg. Chem.* **1986**, *25*, 2074. (d) Kadish, K. M.; Lacombe, D. A.; Anderson, J. E. *Inorg. Chem.* **1986**, *25*, 2246. (e) Kuchynka, D. J.; Amatore, C.; Kochi, J. K. *Inorg. Chem.* **1986**, *25*, 4087. (f) Dessy, R. E.; Weissman, P. M.; Pohl, R. L. *J. Am. Chem. Soc.* **1966**, *88*, 5117.

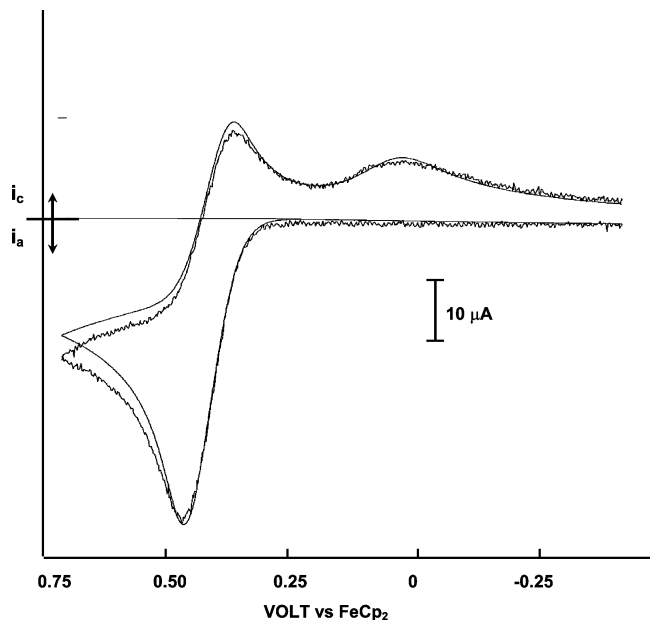
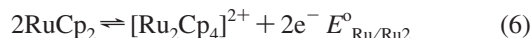


**Figure 3.** Measured (line with noise) and calculated CV scan of 2 mM **1** in  $\text{CH}_2\text{Cl}_2/0.1 \text{ M } [\text{NBu}_4][\text{TFAB}]$  at 2 mm glassy carbon electrode, scan rate  $0.3 \text{ V s}^{-1}$ ,  $T = 256 \text{ K}$ . Experimental curve was background-subtracted and  $iR$ -compensated. Simulation employed  $\text{EC}_{\text{dim}}$  mechanism for the  $1/1^+$  couple ( $E^\circ = 0.41 \text{ V}$ ,  $K_{\text{dim}} = 1 \times 10^4 \text{ M}^{-1}$ ,  $k_{\text{dim}} = 1.5 \times 10^3 \text{ M}^{-1} \text{ s}^{-1}$ ).

(eq 5),<sup>19</sup> the overall agreement was limited by both the challenging experimental conditions and the fact that a unique set of parameters cannot be obtained for the electrochemically irreversible two-electron cathodic reduction of the dimer dication. The best fits employed values of  $K_{\text{dim}}$  that were slightly lower than that ( $K_{\text{dim}} = 9 \times 10^4 \text{ M}^{-1}$  at 243 K) given in our preliminary communication.<sup>13</sup> Reasonable agreements were obtained at 256 K ( $K_{\text{dim}} = 1 \times 10^4 \text{ M}^{-1}$ ,  $k_{\text{dim}} = 1.5 \times 10^3 \text{ M}^{-1} \text{ s}^{-1}$ ) and at 268 K ( $K_{\text{dim}} = 2.5 \times 10^3 \text{ M}^{-1}$ ,  $k_{\text{dim}} = 7 \times 10^3 \text{ M}^{-1} \text{ s}^{-1}$ ), but the accuracies of these values were insufficient to encourage a quantitative interpretation of changes in the dimerization equilibrium constant as a function of temperature. Nevertheless, the order of magnitude of these  $K_{\text{dim}}$  values provides a guide as to the chemical makeup of equilibrated monomer/dimer solutions of  $1^+/2^{2+}$  under these conditions. For example, using a value of  $K_{\text{dim}} = 1 \times 10^4 \text{ M}^{-1}$  at 256 K (see simulation in Figure 3), a nominally 2 mM solution of the ruthenocenium cation would contain 0.36 mM  $1^+$  (18% of the nominal concentration), the remainder existing as the dimer  $2^{2+}$ .

When the  $\text{EC}_{\text{dim}}$  reactions of eqs 3 and 4 are rewritten as the overall redox process of eq 6, it becomes clear that an independent estimate of  $K_{\text{dim}}$  can be made based on the measured potential,  $E^\circ_{\text{Ru/Ru}_2}$ , of the reaction. Making the usual assumptions for the



approximation of  $E^\circ$  by  $E_{1/2}$ ,<sup>20</sup> one obtains an expression (eq 7) relating the measured

$$E_{1/2}(\text{Ru/Ru}_2) = E_{1/2}(\text{Ru/Ru}^+) - RT/nF(\ln K_{\text{dim}}) \quad (7)$$

value,  $E_{1/2}(\text{Ru/Ru}_2)$ , to  $K_{\text{dim}}$  and the potential expected for the one-electron oxidation of ruthenocene (eq 3),  $E_{1/2}(\text{Ru/Ru}^+)$  in the absence of a coupled dimerization. The latter can be estimated as 0.57 V, based on differences in the ionization potentials of ferrocene (6.88 eV)<sup>21</sup> and ruthenocene (7.45 eV)<sup>21</sup> (see Table 1), requiring a value of  $K_{\text{dim}} = 5 \times 10^2 \text{ M}^{-1}$  to account for the measured  $E_{1/2}$  of 0.41 V at 298 K. This estimate is qualitatively consistent with the values ( $10^3$  to  $10^4 \text{ M}^{-1}$ ) determined by the CV simulations at lower temperatures.

It is worth noting that dimerization of the osmocenium ion appears to be less highly favored, at least in a TFAB-containing electrolyte. The potential for the osmocene/osmocenium couple versus ferrocene is within experimental error of the ionization potential difference (Table 1), and no evidence of a dimer product wave was observed even when a 2.5 mM solution of  $\text{OsCp}_2$  was scanned at 233 K. An expanded discussion of the relationship between  $E_{1/2}$  values and ionization potentials of metallocenes is available.<sup>21</sup>

**IB.  $[\text{B}(\text{C}_6\text{H}_3(\text{CF}_3)_2)_4]^-$ .** Changing the electrolyte anion from TFAB to  $\text{BArF}_{24}$  had a noticeable effect on the voltammetric responses of **1**. At room temperature, the reversible one-electron process  $1/1^+$  appeared at the more positive potential of  $E_{1/2} = 0.57 \text{ V}$ , confirming the earlier report of Hill and co-workers.<sup>12,22</sup> In addition, two cathodic product peaks were observed in relative amounts that depended on temperature and CV scan rate. At temperatures below 250 K ( $\nu = 0.3 \text{ V s}^{-1}$ ), the main follow-up product appeared between  $E_{\text{pc}}$  values of  $-0.05$  and  $-0.1 \text{ V}$  (Figure 4). At room temperature, this peak essentially disappeared and was replaced by one at  $E_{\text{pc}} = -0.25$  to  $-0.35 \text{ V}$ . On the basis of NMR studies (vide infra), the product peaks were assigned to  $2^{2+}$  (more positive peak, favored at lower temps) and the dinuclear complex  $3^{2+}$  (more negative peak, favored at higher temps). An attractive feature of the  $\text{BArF}_{24}$ -electrolyte solutions was that the products were sufficiently soluble to remain in solution at the low temperature which had caused precipitation of  $[\text{2}][\text{TFAB}]_2$  when TFAB was the electrolyte anion. This greater solubility facilitated in situ NMR identification of the electrolysis products.

**II. Addition of  $[\text{PF}_6]^-$  Electrolyte.** The addition of even small amounts of  $[\text{NBu}_4][\text{PF}_6]$  to a solution of **1** in  $[\text{NBu}_4][\text{TFAB}]$  or  $[\text{NBu}_4][\text{BArF}_{24}]$  had an immediate effect on the chemical reversibility of the ruthenocene oxidation.

(20) The use of  $E_{1/2}$  in place of  $E^\circ$  values assumes that the activity and diffusion coefficients for Ox and Red are equal in the experimental medium. Under our conditions, potential differences of 10 mV or less are expected.

(21) Ryan, M. F.; Richardson, D. E.; Lichtenberger, D. L.; Gruhn, N. E. *Organometallics* **1994**, *13*, 1190.

(22) Although this value is precisely that expected based on the ionization potential of ruthenocene,<sup>21</sup> implying by the earlier reasoning that the dimerization equilibrium constant,  $K_{\text{dim}}$ , may be lower when  $\text{BArF}_{24}$  is the counteranion, we have no direct confirmation of this.

(19) The reduction of  $2^{2+}$  is likely, in fact, to proceed by an  $\text{E}_{\text{irrev}}\text{CE}_{\text{rev}}$  process in which the first one-electron process results in cleavage of the Ru–Ru bond and production of 1 equiv each of ruthenocene and ruthenocenium ion, the second of which would be immediately reduced at the potential of its generation.

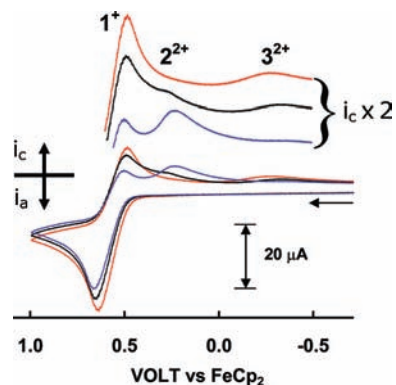


**Figure 4.** CVs of 2 mM  $\text{CH}_2\text{Cl}_2$  solutions of **1** in the presence of 0.1 mM  $[\text{NBu}_4][\text{B}(\text{C}_6\text{H}_3(\text{CF}_3)_2)_4]$  at 298 K (red, largest feature), 268 K (black), and 250 K (blue) at a scan rate of  $0.3 \text{ V s}^{-1}$ . The inset shows a double magnification of the cathodic waves. The general positions of the cathodic waves of  $1^+$ ,  $2^{2+}$ , and  $3^{2+}$  are shown.

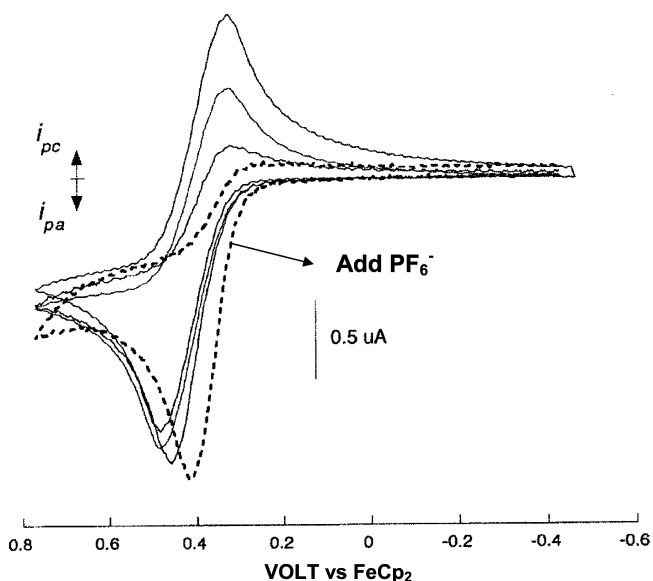


**Figure 5.** CV scans showing effect of successive additions of  $[\text{NBu}_4][\text{PF}_6]$  to a solution of 2.2 mM **1** in  $\text{CH}_2\text{Cl}_2/0.1 \text{ M } [\text{NBu}_4][\text{TFAB}]$  at 2 mm glassy carbon electrode, scan rate  $0.2 \text{ V s}^{-1}$ ,  $T = \text{ambient}$ . The three successive additions were of 0.5, 1, and 10 equiv of  $[\text{PF}_6]^-$ .

As shown in Figure 5, by the time 10 equiv of  $[\text{PF}_6]^-$  had been added, the oxidation of **1** had lost all chemical reversibility. The negative potential shift is consistent with either a coupled follow-up reaction or an increased ion pairing of  $1^+$  with  $[\text{PF}_6]^-$ . The follow-up product in this case is most likely a metal-fluoride or metal-F- $\text{PF}_5$  Ru(IV) complex, but no attempts were made to identify it. Addition of small amounts of nitromethane, acetonitrile, moisture, or oxygen to  $[\text{NBu}_4][\text{BARF}_{24}]$  solutions of anodically electrolyzed ruthenocene immediately produced a red solution which is likely to be associated with formation of one or more Ru(IV) complexes. It has been previously shown that the product of the chemical oxidation of osmocene in acetonitrile is the Os(IV) complex  $[\text{Cp}_2\text{Os}(\text{NCCH}_3)][\text{PF}_6]_2$ .<sup>14</sup> The osmocene analogues of  $2^{2+}$  and even  $4^{2+}$  are, however, stable toward nitromethane, unlike the present ruthenium-containing dimer  $2^{2+}$  or the Ru dinuclear species  $3^{2+}$ .

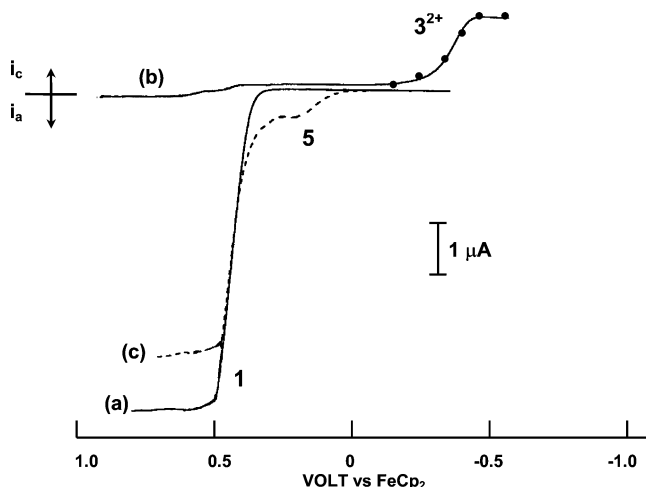
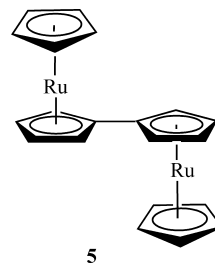


**Figure 6.** Linear scan voltammograms ( $5 \text{ mV s}^{-1}$ ) of three stages of bulk electrolysis of 5 mM **1** in  $\text{CH}_2\text{Cl}_2/0.1 \text{ M } [\text{NBu}_4][\text{TFAB}]$ ,  $T = 233 \text{ K}$ : (a) prior to electrolysis, (b) after exhaustive bulk electrolysis at  $E_{\text{appl}} = 0.7 \text{ V}$ , (c) after exhaustive re-reduction at  $E_{\text{appl}} = -0.6 \text{ V}$ .

**Electrochemistry on Electrolysis Time Scale in WCA Electrolytes.** With TFAB as the electrolyte anion, bulk electrolysis at 243 K passed exactly one faraday and most of the dimer  $2^{2+}$  precipitated as a pure yellow  $[\text{TFAB}]_2$  salt. Owing to the product precipitation, linear scans of the solution after electrolysis [scan (b) in Figure 6] only had very small cathodic contributions arising from  $1^+$  and  $2^{2+}$ . However, this same scan revealed the presence of a more soluble second product having  $E_{1/2}$  of  $-0.35 \text{ V}$  (note section with solid circles,  $\text{---}\bullet\text{---}\bullet\text{---}\bullet\text{---}$ , in Figure 6) which is assigned to the dimetallated complex  $3^{2+}$ . When this solution was re-electrolyzed at a potential negative of this second product ( $E_{\text{appl}} = -0.6 \text{ V}$ ), about 80% of the original wave for **1** was regenerated [see dashed line (c) in Figure 6], as the reduction of both  $2^{2+}$  and  $3^{2+}$  gave back ruthenocene, the first of these slowly redissolving as it was reduced. The small wave at  $E_{1/2} = 0.25 \text{ V}$  (reversible by CV) is ascribed to biruthenocene, **5**, by the matching of its potential to that of an authentic sample.<sup>23</sup> This minor product appeared to varying degrees in electrolyses at different concentrations and temperatures, never accounting for more than about 13% of the sum of currents for all the final products. The possible origin of this side product is discussed later.



(23) The reversible two-electron oxidation of **5** in  $\text{CH}_2\text{Cl}_2/0.1 \text{ M } [\text{NBu}_4][\text{ClO}_4]$  has been reported in Watanabe, M.; Sato, M.; Takayama, T. *Organometallics* **1999**, *18*, 5201. The oxidation product is a fulvalenyl-type isomer of  $3^{2+}$ ,  $[\text{Ru}_2\text{Cp}_2(\mu_2\text{-}\eta^6\eta^6\text{-C}_{10}\text{H}_8)]^{2+}$ . We thank Dr. Masaru Sato (Saitama University) for a sample of biruthenocene and Derek Laws (University of Vermont) for determining its potential in WCA media.

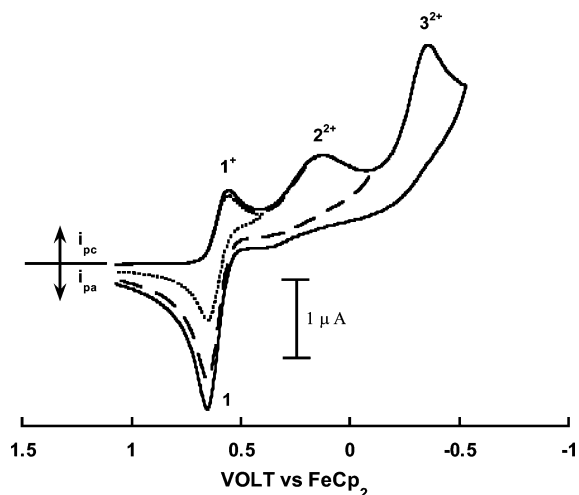


**Figure 7.** Cyclic voltammograms scanned to three different switching potentials after exhaustive anodic oxidation of 5 mM **1** in  $\text{CH}_2\text{Cl}_2/0.05 \text{ M}$   $[\text{NBu}_4][\text{BArF}_{24}]$  at  $T = 243 \text{ K}$ , scan rate  $0.1 \text{ V s}^{-1}$ , 1 mm glassy carbon electrode. Adapted with additions from ref 13.

The partial precipitation of  $2[\text{TFAB}]_2$  at low temperatures presented a complication in our efforts to characterize the structures of the dinuclear products by NMR spectroscopy. Fortunately, the anodic products exhibited greater solubilities as  $\text{BArF}_{24}$  salts. This is well demonstrated by CVs after the low-temperature bulk oxidation of ruthenocene in  $[\text{NBu}_4][\text{BArF}_{24}]$  (Figure 7), for which the three cathodic waves were assigned to reduction of  $1^+$ ,  $2^{2+}$ , and  $3^{2+}$ , all of which reproduced **1** in the process of a cathodic back-electrolysis at  $E_{\text{appl}} = -0.6 \text{ V}$ .

**$^1\text{H}$  NMR of Bulk Electrolysis Products.** For in situ NMR-characterization of the solution generated by low-temperature anodic electrolysis of **1**, a low concentration of electrolyte was used to facilitate NMR shimming and to minimize the  $^1\text{H}$  resonance features of the  $[\text{NBu}_4]^+$  and  $[\text{B}(\text{C}_6\text{H}_3(\text{CF}_3)_2)_4]^-$  ions. The most common condition of about 10 mM **1** and 40 mM  $[\text{NBu}_4][\text{B}(\text{C}_6\text{H}_3(\text{CF}_3)_2)_4]$  in 2–4 mL  $\text{CD}_2\text{Cl}_2$  at 233 K required long electrolyses times (over 1 h; see Experimental Section) that were terminated before completion, complicating the spectra owing to the presence of a certain amount of unreacted **1** ( $\delta = 4.5 \text{ ppm}$  for pure **1**). Under these long electrolysis conditions a peak was also observed at  $\delta = 5.95 \text{ ppm}$  which did not vary with the NMR temperature and which was assigned to a Ru(IV) side product.<sup>24</sup> In spite of the complications, these experiments provided valuable information in delineating the makeup of the post-electrolysis solutions.

The  $^1\text{H}$  NMR spectra of the electrolysis solutions were reversibly temperature sensitive (303 to 223 K), with the most important features being shown in Figure 8. In the spectrum taken at 228 K, the singlet at  $\delta = 5.38$ , directly to the low-field side of the  $\text{CDHCl}_2$  peak, is assigned to the dimer  $2^{2+}$  (the osmium analogue of this compound,

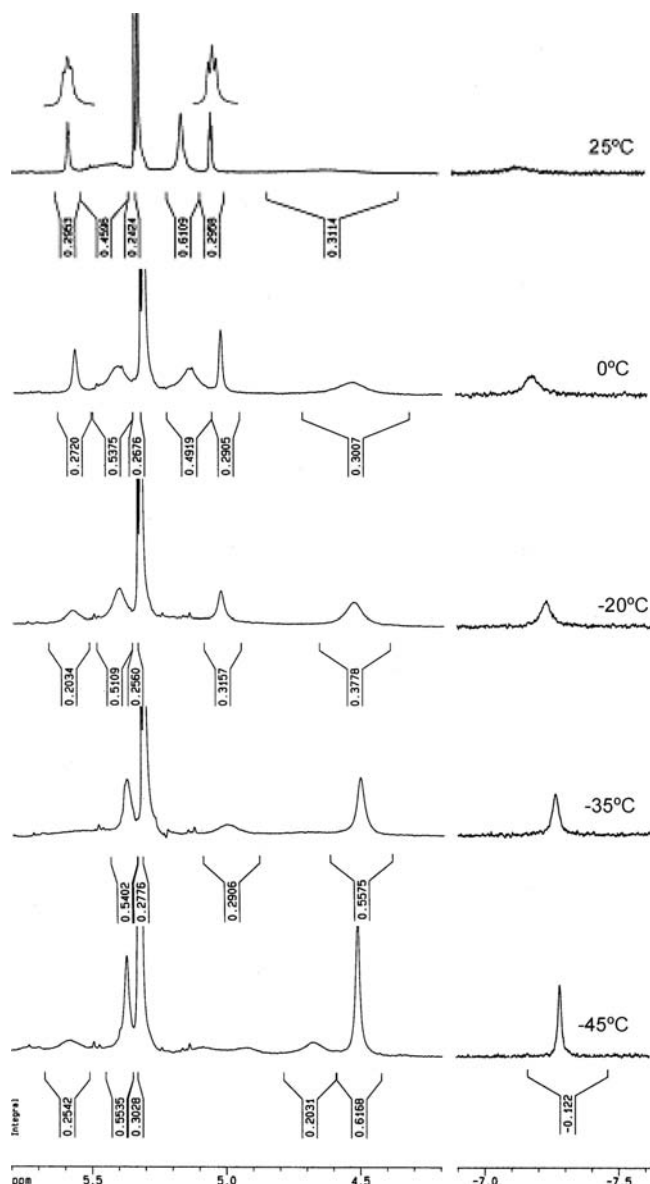


**Figure 8.**  $^1\text{H}$  NMR of the equilibrium behavior system of electrochemically oxidized **1** at the indicated temperatures highlighting the collapse of triplet signals at 5.53 (2H) and 5.02 (2H) ppm and the singlet at 5.14 (5H) ppm of **3** at 25 °C into a singlet at 5.38 ppm for the equivalent  $4 \times (\text{C}_5\text{H}_5)$  protons of  $2^{2+}$  at  $-45 \text{ }^\circ\text{C}$ . The singlet signal at 4.5 ppm that is associated with **1** disappeared because of fast exchange with  $1^+$  at 25 °C. The hydride signal at  $-7.1$  to  $-7.3 \text{ ppm}$  is associated with  $(\mathbf{1-H})^+$  that may form according to eq 9.

$[\text{Os}_2\text{Cp}_4]^{2+}$ , was found at 5.89 ppm<sup>14</sup>). This singlet broadens strongly at higher temperatures owing to two coupled reactions in which the dimer dication is increasingly disfavored: the monomer–dimer equilibrium,  $2\mathbf{1}^+ \rightleftharpoons 2^{2+}$ , and the reversible formation of the dinuclear complex  $3^{2+}$  from  $2^{2+}$ . Evidence for  $3^{2+}$  will be presented below. Consistent with the influence of the monomer/dimer equilibrium,  $1^+/2^{2+}$ , is the effect on the ruthenocene Cp-resonance (4.5 ppm at 223 K) which broadens to the point of disappearance at higher temperatures because of Heisenberg broadening through self-exchange<sup>25</sup> between the ruthenocenium ion and the unreacted ruthenocene.

Coincident with the loss of intensity for  $2^{2+}$  at higher temperatures is the onset of a pair of triplets at  $\delta = 5.53$

(24) The electrolysis solution took on a reddish cast late in the electrolysis, a color that was immediately produced if a solution of the products was treated with acetonitrile or exposed to air. Formal Ru(IV) organometallic complexes such as  $[\text{RuCp}_2\text{I}]_3$  (reference 9) are generally red. See also Borrell, P.; Henderson, E. *J. Chem. Soc., Dalton Trans.* **1975**, 432.

and 5.02 as well as a singlet at 5.14 which integrate to 2:2:5, respectively. These peaks are assigned to the complex  $3^{2+}$  in which two cyclopentadienyl rings are sigma-bonded to metal centers, analogous to the dimetallic osmium complex,  $4^{2+}$ , identified earlier by both  $^1\text{H}$  NMR spectroscopy [ $\delta = 6.19$  (t), 5.27 (t), and 5.91 (s)] and by X-ray crystallography.<sup>14</sup> The other possible structure that would be consistent with this set of resonances, namely biruthenocene ( $5$  or  $5^{2+}$ ), is ruled out owing to the fact that the cathodic CV curve for the major room-temperature product is highly irreversible, consistent with the expected cathodic behavior of  $3^{2+}$ , but inconsistent with the reversible CV redox behavior observed for  $5^{2+}/5$ .<sup>23</sup> Furthermore, the  $^1\text{H}$  NMR literature values for  $5$  are  $\delta = 4.68$  (t), 4.44 (t), and 4.48 (s) in  $d^6$ -acetone.<sup>26</sup>

The question of what happens to the two H-atoms lost from the Cp ligands of the dimer  $2^{2+}$  is addressed in eqs 8 and 9. Droegge et al. postulated an irreversible version of eq 8 to account for the slow spontaneous reaction of  $[\text{Os}_2\text{Cp}_4][\text{PF}_6]_2$  to give  $4^{2+}$  as well as



osmocene and  $\text{H}[\text{PF}_6]$ .<sup>14</sup> Equation 9 takes into account the possible formation of ruthenocene hydride under these conditions. Referring again to Figure 8, a hydride resonance is indeed seen at  $\delta$  values between  $-7.1$  and  $-7.3$  ppm, becoming sharper at lower temperatures. The final expected spectral feature, namely, that of the cyclopentadienyl rings of  $1\text{-H}^+$ , appears to be a singlet for which the resonance position is highly temperature sensitive. This line, pointed out in the arrows of Figure 9, was found between about 1.8 (298 K) and 3.7 ppm (228 K) and, wherever possible to integrate against the metal-hydride peak,<sup>27</sup> was 10 times its intensity. Although it is unclear why the Cp resonance of  $1\text{-H}^+$  varies so much in chemical shift, its position may be affected by the self-exchange reaction between  $1^+$  and  $1$  or by fluxionality in the ring-hydrogen–metal interaction. The structures possible for protonated ruthenocene have received theoretical and experimental attention but not under the medium conditions of the present study. Gas-phase calculations indicated that the metal-protonated form of  $[\text{RuC}_{10}\text{H}_{11}]^+$  (below) was energetically preferred over the ring-protonated or agostic form,<sup>28</sup> but changes in solvent and counteranion have been shown to affect the favored structure in lower

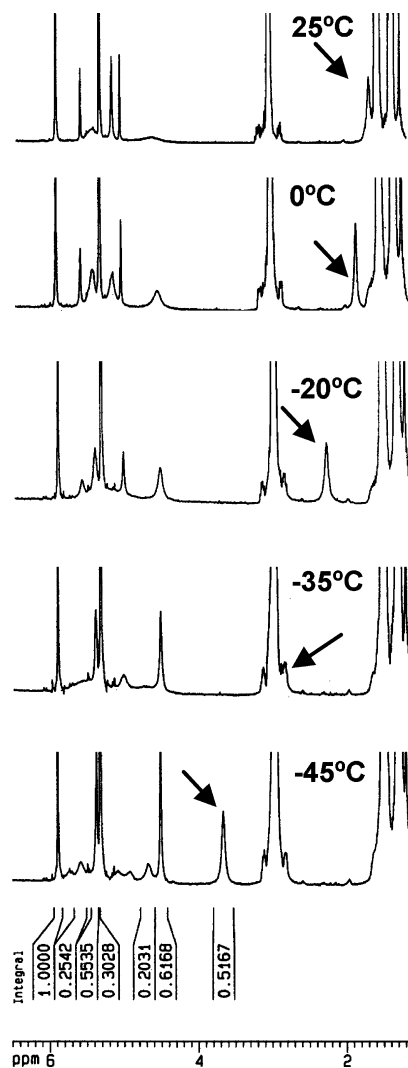
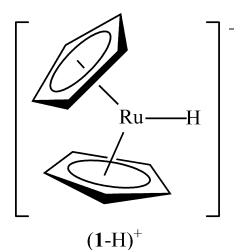


**Figure 9.** Fragments of  $^1\text{H}$  NMR spectra highlighting the wandering singlet peak associated with the  $\text{C}_5\text{H}_5$  groups of  $1\text{-H}^+$  as a function of temperature.



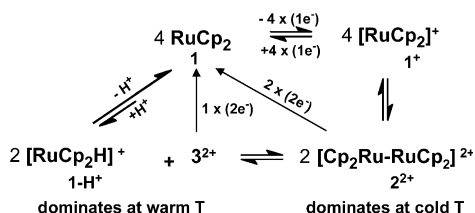
polarity media<sup>29</sup> (structural aspects of the comparatively well-studied ferrocene hydride are still being debated).<sup>30</sup> The high acidity of acids of weakly coordinating anions<sup>31</sup> assures the high activity of protons in a dichloromethane/ $[\text{BARF}_{24}]$  medium.

- (25) NMR-line broadening has been well characterized for ferrocene/ferrocenium and for other metallocene redox mixtures. For leading references see (a) Zahl, A.; van Eldik, R.; Matsumoto, M.; Swaddle, T. W. *Inorg. Chem.* **2003**, *42*, 3718. (b) Blümel, J.; Hebenand, N.; Hudeczek, P.; Köhler, F. H.; Strauss, W. *J. Am. Chem. Soc.* **1992**, *114*, 4223. (c) Nielson, R. M.; McManis, G. E.; Safford, L. K.; Weaver, M. J. *J. Phys. Chem.* **1989**, *93*, 2152. (d) Nielson, R. M.; McManis, G. E.; Golovin, M. N.; Weaver, M. J. *J. Phys. Chem.* **1988**, *92*, 3441.
- (26) Watanaba, M.; Iwamoto, T.; Hirotschi, S.; Motoyama, I. *J. Organomet. Chem.* **1993**, *446*, 177.
- (27) Integrations were carried out on the spectra at 273 K, 253 K, and 228 K by a manual (cut and weigh) method that we estimate to have a relative error of about 10%.
- (28) Borisov, Yu. A.; Ustynyuk, N. A. *Russ. Chem. Bull., International Ed.* **2002**, *51*, 1900.

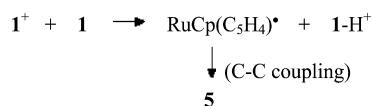
- (29) Shubina, E. S.; Krylov, A. N.; Kreindlin, A. Z.; Rybinskaya, M. I.; Epstein, L. M. *J. Organomet. Chem.* **1994**, *465*, 259.
- (30) For recent papers see (a) Bühl, M.; Grigoleit, S. *Organometallics* **2005**, *24*, 1516. (b) Mayor-López, M. J.; Lüthi, H. P.; Koch, H.; Morgantini, P. Y.; Weber, J. *J. Chem. Phys.* **2000**, *113*, 8009.
- (31) (a) Reed, C. A.; Kim, K. C.; Bolskar, R. D.; Mueller, L. J. *Science* **2000**, *289*, 101. (b) Jutzi, P.; Müller, C.; Stämmler, A.; Stämmler, H.-J. *Organometallics* **2000**, *19*, 1442. (c) Brookhart, M.; Grant, B., Jr. *Organometallics* **1992**, *11*, 3920.



## Scheme 1



## Scheme 2



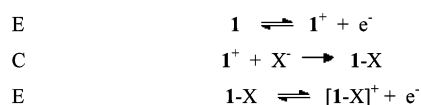
Given the complexity of the processes in eqs 8 and 9, we wish to emphasize the exactly reproducible  $^1\text{H}$  NMR spectra as the sample temperature was cycled as many as three times between 228 and 298 K. The optimum temperature range for simultaneous detection of the two dinuclear species,  $\mathbf{2}^{2+}$  and  $\mathbf{3}^{2+}$ , was 253 to 273 K, a result which is consistent with the simultaneous cyclic voltammetric detection of  $\mathbf{2}^{2+}$  and  $\mathbf{3}^{2+}$  at 268 K (Figure 4).

The reactions of the ruthenocenium ion under these electrolytic conditions are therefore dominated by the processes in Scheme 1. Owing to the high reactivity of  $\mathbf{1}^+$ , side reactions not shown in Scheme 1 also come into play, albeit in relatively unimportant roles. Thus, a small amount of an unknown, likely mononuclear, Ru(IV) product is formed, and it is also possible that some ruthenocene hydride,  $\mathbf{1}\text{-H}^+$ , appears owing to an unspecified H-atom abstraction, perhaps from trace moisture, by the ruthenocenium ion. A possible explanation for the fact that both  $\mathbf{1}\text{-H}^+$  and the fulvalendiyl complex  $\mathbf{5}$  appear in long-term electrolyses (the latter as a low-yield side product) is given in Scheme 2. This scheme considers the possibility of H-atom transfer from  $\mathbf{1}$  to  $\mathbf{1}^+$ , giving a neutral cyclopentadienyl radical that would undergo C–C coupling to form  $\mathbf{5}$ .

**Summary.** The present work corroborates the idea<sup>12,13</sup> that the oxidation of ruthenocene is intrinsically a quasi-Nernstian one-electron process. The ruthenocenium ion is certainly a stronger one-electron oxidant than the ferrocenium ion owing to its more positive  $E_{1/2}$  value (0.41 V in  $\text{CH}_2\text{Cl}_2/[\text{NBu}_4][\text{TFAB}]$ ). However, its tendency to form an 18-electron complex is dominated less by simple electron transfer than by acquisition of a one-electron ligand by the metal center, which is much more capable of expanding its coordination number than is the iron atom of ferrocenium. The present work shows that Ru–Ru, Ru–( $\sigma$ )C, and Ru–H containing complexes (see  $\mathbf{2}^{2+}$ ,  $\mathbf{3}^{2+}$ , and  $\mathbf{1}\text{-H}^+$ , respectively), may all exist under gentle medium conditions. The bonding interactions are sufficiently weak to allow reversible transformations involving several of these species with changes in temperature, concentration, and identity of the counterion. Although these transformations may involve intermolecular H-atom transfers, their mechanisms are still open to question.

The present observations help elucidate the processes responsible for the previously reported products, namely, the Os analogues of  $\mathbf{2}^{2+}$  and  $\mathbf{3}^{2+}$ , isolated after the chemical oxidation of osmocene by  $\text{Ce}^{4+}$ .<sup>14</sup> Formation of the very

## Scheme 3



similar doubly metallated complex  $\text{Re}_2\text{Cp}_2(\sigma\text{:}\eta^5\text{-C}_5\text{H}_4)_2$  by a thermal reaction of the rhenocene dimer,  $\text{Re}_2\text{Cp}_4$ ,<sup>32</sup> also fits into this general class of reactions, as Re(II) is iso-electronic with Os(III). Dinuclear complexes containing  $\sigma\text{:}\eta^5\text{-C}_5\text{H}_4$ -bonded ligands have also been reported for earlier second and third-row metals such as Nb, Mo, and W.<sup>33</sup>

The fact that Ru(IV) product compounds have often been observed after either chemical or electrochemical oxidation of ruthenocene has generally been attributed to a direct disproportionation of the formally Ru(III) ruthenocenium ion (eq 2).<sup>4,6–9,34</sup> The disproportionation equilibrium constant,  $K_{\text{disp}}$ , is not likely to be high enough, however, to support this mechanism.<sup>35</sup> A more likely occurrence is the ECE process of Scheme 3. In this mechanism, the ruthenocenium ion reacts with a nucleophile  $\text{X}^-$  to form a neutral Ru<sup>III</sup>-X complex which undergoes a further one-electron oxidation to give the final  $[\text{Ru}^{\text{IV}}\text{-X}]^+$  product. The requirement that  $E_{1/2}$  for the oxidation of  $\text{RuCp}_2\text{X}$  must be more negative than the value for  $\text{RuCp}_2$  seems reasonable, and a mechanism of this type has been postulated for the oxidation of ruthenoceneophanes in acetonitrile.<sup>36</sup>

Returning to the possibility of employing the second and third-row metallocenes as molecular redox tags, the fact that the 17-electron complexes of the heavier metals are much more reactive than the ferrocenium ion will certainly limit the ways in which the  $\text{MCp}(\eta^5\text{-C}_5\text{H}_4)$  moiety ( $\text{M} = \text{Ru}, \text{Os}$ ) can be employed. However, the increased ability of the heavier metals to reach the inert gas configuration by expanding their coordination spheres may, in fact, be useful in designing synthetic or catalytic uses for compounds having these metallocenyl moieties. Some work along these lines has already appeared.<sup>37</sup> Furthermore, in situations where  $\text{MCp}(\eta^5\text{-C}_5\text{H}_4)$  moieties are in fixed positions and free of

(32) Pasmán, P.; Snel, J. J. M. *J. Organomet. Chem.* **1984**, *276*, 387.

(33) (a) Barral, M. C.; Green, M. L. H.; Jimenez, R. *J. Chem. Soc., Dalton Trans.*, 1982, 2495. (b) Bashkin, J.; Green, M. L. H.; Poveda, M. L.; Prout, K. J. *J. Chem. Soc., Dalton Trans.*, 1982, 2485. (c) Guggenberger, L. J. *Inorg. Chem.* **1973**, *12*, 294. (d) Guggenberger, L. J.; Tebbe, F. N. *J. Am. Chem. Soc.* **1971**, *93*, 5924.

(34) (a) Banks, C. E.; Robinson, K. L.; Liang, H.-P.; Meredith, A. W.; Lawrence, N. S. *Electroanalysis* **2007**, *19*, 555. (b) Lawrence, N. S.; Banks, C. E.; Tustin, G. J.; Jones, T. G. J.; Smith, R. B.; Davis, J.; Wadhawan, J. D. *Electrochem. Commun.* **2007**, *9*, 1451.

(35) Although the direct disproportionation of  $\mathbf{1}^+$  cannot be ruled out as being responsible for Ru(IV) side products, this is unlikely based on the very unfavorable upper limit of  $K_{\text{disp}}$  (eq 2,  $K_{\text{disp}} = [\mathbf{1}^{2+}][\mathbf{1}]/[\mathbf{1}^+]^2$ ) that is apparent from the voltammetric data. The fact that the second oxidation of ruthenocene was not observed within the voltammetric window of our measurements assures that  $E_{1/2}$  for  $[\text{RuCp}_2]^{2+/+}$  is greater than about 1.7 V vs ferrocene. The  $K_{\text{disp}}$  for ruthenocenium ion in this medium must therefore be less than about  $10^{-22}$ .

(36) Hashidzume, K.; Tobita, H.; Ogino, H. *Organometallics* **1995**, *14*, 1187. See also Watanabe, M.; Sato, M.; Nagasawa, A.; Kai, M.; Motoyama, I.; Takayama, T. *Bull. Chem. Soc. Jpn.* **1999**, *72*, 715.

(37) (a) Sato, M.; Nagata, T.; Tanemura, A.; Fujihara, T.; Kumakura, S.; Unoura, K. *Chem.—Eur. J.* **2004**, *10*, 2116. (b) Watanabe, M.; Sato, M.; Takayama, T. *Organometallics* **1999**, *18*, 5201. (c) Sato, M.; Kawata, Y.; Kudo, A.; Iwai, A.; Saitoh, H.; Ochiai, S. *J. Chem. Soc., Dalton Trans.* **1998**, 2215.

### *One-Electron Oxidation of Ruthenocene*

interactions with strong nucleophiles, such as in some solid-state or immobilized molecular applications, ruthenocenyl or osmocenyl-groups have the possibility of functioning as essentially Nernstian one-electron redox agents.

**Acknowledgment.** We gratefully acknowledge the support of the National Science Foundation at the University of Vermont (CHE 04-11703 and CHE 08-08909), the South

African National Research Foundation (2054243), and the Central Research Fund of the University of the Free State. We also thank Boulder Scientific Co., Boulder, Colorado, for a partial donation of electrolyte anions, Dr. Masaru Sato (Saitama University) for a sample of **5**, and Derek Laws (University of Vermont) for experimental assistance.

IC802105B